PROJECT TITLE:

TRANSFORMATION OPTICS FOR ENHANCING LENS-BASED PARALLEL-PLATE WAVEGUIDE BEAM FORMERS

Scientific Report on the Research Activity within the framework

of the ESF program entitled "New Frontiers in Millimetre/Sub-Millimetre

Waves Integrated Dielectric Focusing Systems"

SENDING INSTITUTION:	HOST INSTITUTION:
Institut d'Electronique et des Télécommunications de Rennes (IETR), UMR CNRS 6164, Université de Rennes 1 35042, RENNES, FRANCE	Electromagnetic Engineering (ETK), School of Electrical Engineering (EES) KTH Royal Institute of Technology Teknikringen 33, SE-100 44 Stockholm, SWEDEN
People Involved: Cheikh-Dieylar DIALLO Pr. Ronan SAULEAU	**People Involved:** Dr. Oscar QUEVEDO-TERUEL Mahsa Ebrahimpouri HAMIKAR Dr. Guido VALERIO

Total Time duration: 9 weeks (23/03/2015-22/05/2015)

1. Transformation Optics

Transformation optics (T.O.) is an analytical technique to calculate the material permittivity and permeability tensors that will bend the electromagnetic fields in a prescribed manner, [1] and [2]. This new wave-material interaction provides a pathway to design unprecedented microwave devices, especially T.O. lenses with enhanced performances compared to classical lenses.

The objectives of this mission were to 1) learn and master the T.O. technique and to 2) design an optically transformed lens with enhanced performances compared to classical lens. As regards to the first objective, have been achieved (1.1) a brief study of the literature, (1.2) an analytical and (1.3) a quasi-conformal (non-analytical) transformation based on literature. Eventually, as regards the second objective, (2.1) a parabolic reflector have been flattened, and it has been started (2) a T.O. based extension of a Luneburg lens radiating aperture for beam forming applications.

1. T.O. design methodology and process

T.O. design methodology is based on form-invariant Maxwell's equations. Indeed, in any coordinate system, they can be written as: $\nabla \times \vec{H} = j\omega[\epsilon]\vec{E}$ and $\nabla \times \vec{E} = -j\omega[\mu]\vec{H}$. In a different coordinate system, the form of the equations remains the same ($\nabla' \times \overrightarrow{H'} = j\omega[\epsilon']\overrightarrow{E'}$ and $\nabla' \times \overrightarrow{E'} = -j\omega[\mu']\overrightarrow{H'}$). However the transformation is absorbed by the material parameters as: $[\mu'] = \frac{[A][\mu][A]^T}{\det[A]}$ and $[\epsilon'] = \frac{[A][\epsilon][A]^T}{\det[A]}$, where $[A]$is the Jacobian transformation matrix from the initial coordinate system to the final one.

The design procedure of a T.O. device can be divided into four steps using spatial transforms [3]:

1) Definition of a spatial or coordinate transformation , i.e. from one space to another, one coordinate system to another,
2) Computation of effective material properties,
3) Mapping of material properties to engineered materials,
4) Generation of the overall lattice.

A coordinate transformation is a mapping from one space with a first coordinate system to another space with a second coordinate system. The transformation is described by the Jacobian transformation matrix,$[A]$, in which each term quantifies the "stretching" or the "compression" of the coordinates.

2. Analytic transformation

The following analytical transformation [3] consists of a symmetric centered compression of the Cartesian coordinate system along the y-axis, as show in **Fig. 1**, **Fig. 2** and **Fig. 3**. From the equations, we have calculated the 9 elements of the material parameters, $[\epsilon]$ and$[\mu]$. Then, we have implemented the element equations in a Matlab code. They are showed in Fig. 4, Fig. 5 and Fig. 6. Compared to [3], the results are in good agreement, except that we do not know the values of σ_x and σ_y the author used.

$$x' = x$$

$$y' = \left[1 - exp\left(-\frac{x^2}{{\sigma_x}^2} - \frac{y^2}{{\sigma_y}^2}\right)\right]$$

$$z' = z$$

Fig. 1 Equations of the « squeezing » transformation [3]

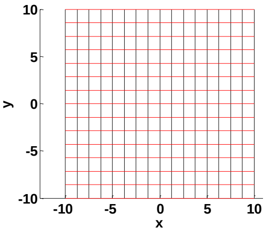

Fig. 2 Rays are straight lines in the Cartesian system

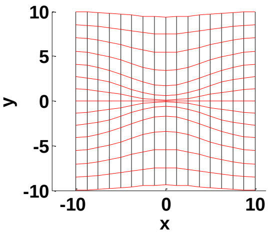

Fig. 3 Rays are squeezed lines in the new coordinate system

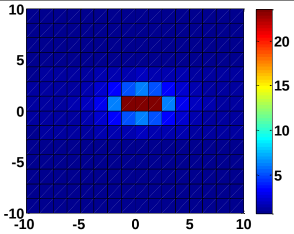

Fig. 4 μ_{xx}

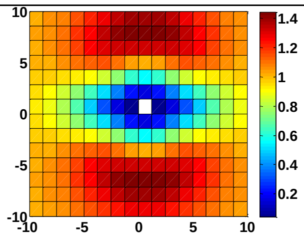

Fig. 5 μ_{yy}

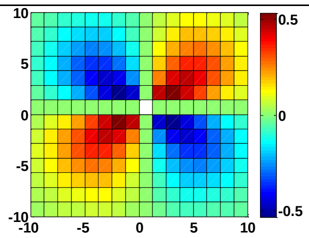

Fig. 6 μ_{xy}

3. Quasi-Conformal T.O.

The transformation used in the previous section is analytical, meaning that it can be found an analytical expression of the effective material tensors. Besides, the material found is anisotropic. In T.O. design, it is not always possible to find an analytic expression of the transformation, and anisotropic materials are avoided because of their dispersion and their complex manufacturing. A quasi-conformal T.O. [4] (QCTO) is a solution for non-analytical T.O. design and it gives isotropic material.

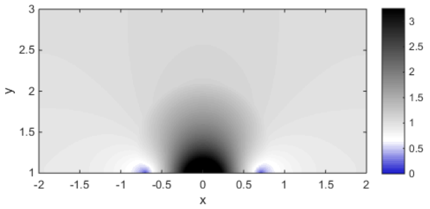

Fig. 7 Permittivity map

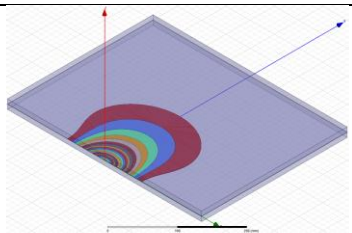

Fig. 8 Transformed lens drawn in HFSS

During this mission we retrieve the same results as [5], where a Luneburg lens have been flattened using T.O. giving more than full decade bandwidth and almost 180° field-of-view. To do that we learned how to generate orthogonal grids with the mesher PointWise [6], draw the geometry contour in the mesher then imported the coordinate data in a Matlab code. There, we implemented the QCTO and retrieved the permittivity map, shown in Fig. 7. Finally, as shown in Fig. 8 we drew the 2D model in commercial softwares (HFSS, CST).

4. Parabolic Reflector

In the two previous sections, we have studied two literature cases. In order to complete the first objective of the mission, we decided to design a new T.O. based device, which is a parabolic reflector flattened with T.O. The reference parabola was taken from [7]. And this transformation aimed at reducing space. We draw the geometry, Fig. 9 , in Pointwise, and from it we imported the orthogonal grid in Matlab. Then we computed the permittivity map and generated the contours in Matlab and in CST, Fig. 10. Finally we simulated successfully the parabola between 22 GHz and 30 GHz, **Fig. 11**.

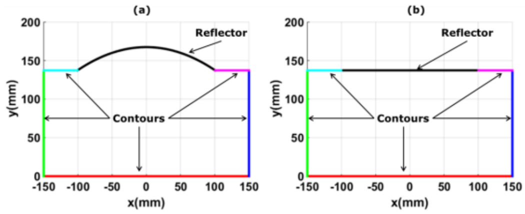

Fig. 9 Geometry of the transformation. (a) Virtual space. (b) Real space

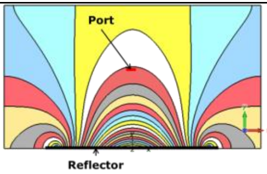

Fig. 10 CST model of the flattened parabola

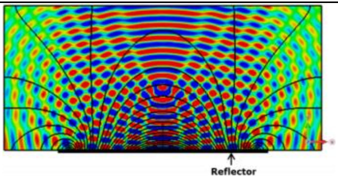

Fig. 11 E Field distribution at 24 GHz

5. Luneburg lens radiating aperture extension

The second and final objective of this mission was to use T.O. to design an innovative lens. Fig. 12 is depicted a pillbox quasi-optical beamformer. The current approach to decrease the size of this type of beamformer is to fill it with high permittivity. However, a physical connection is required between beam ports of the beamformer and the radiating element of the array. So a sampling of the wave is then enforced, which limits the scan range of the radiating aperture, as well as the operating bandwidth. A solution to this limit is to use T.O. technique to conceive a smooth transition between a compact Luneburg beamformer and a continuous linear radiating aperture.

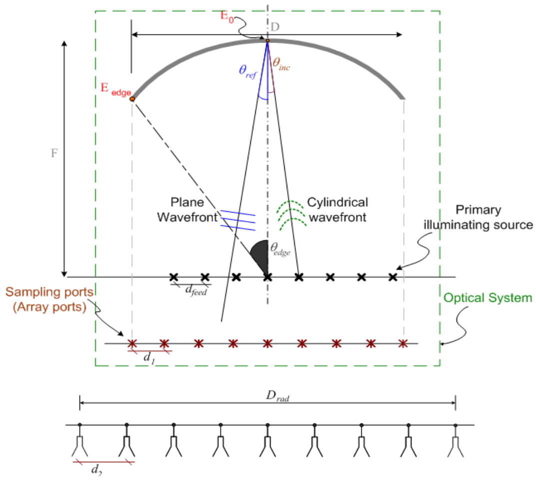

Fig. 12 Pillbox quasi-optical beamformer

i. Outer lens transformation

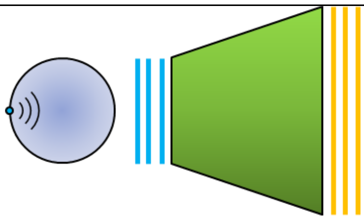

Fig. 13 Smooth T.O. transition between the outer space of the lens and the radiating elements

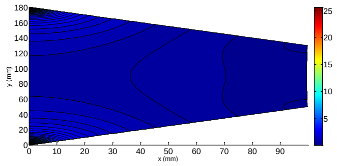

Fig. 14 Discretization of permittivity map

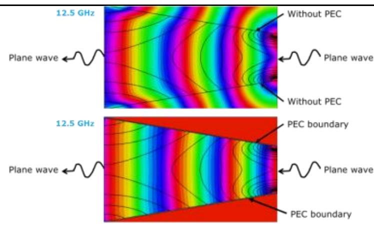

Fig. 15 E fields distribution in the transformed space

The first solution we considered was to transform only the space after the Luneburg lens, as depicted in green Fig. 13. This transformation looks like the one performed in [8]. The permittivity map is shown in Fig. 14. The permittivity ranges from 1 to 25 because of the edges. Therefore it is better to choose a transformed space without edges. Fig. 15 shows the plane phase fronts coming out of the Luneburg lens and going into the transformed space. The wave is going out from this space still plane, especially when the transformed space is bound by metal plates (PEC). Besides the dramatic change of permittivity, in this first solution the amplitude of the plane wave are not uniform at the aperture, it is concentered in the center. So we consider as a second solution the transformation of the inner space of lens besides the outer space.

ii. Inner and outer lens space transformation

The second solution considered for beamformer radiating aperture extension was to transform the lens and the space after it, as illustrated in **Erreur ! Source du renvoi introuvable.**. For that we started from a Luneburg lens of diameter 240 mm at 12.5 GHz, which would give the desired radiating aperture width. The idea is to transform it into a smaller Luneburg lens but with the same radiating aperture width, at the expense of permittivity change of the real space. The spatial transformation is described in Fig. 17. So the N_2points in the virtual space have to be mapped to N_2points of the real space, in **Erreur ! Source du renvoi introuvable.**. With the mesher PointWise we generated the quasi-orthogonal grid, necessary for a QCTO, of the virtual space, **Fig. 18**. However with PointWise we dit not find a way to do the same with the real space, i.e. generate an orthogonal grid for the real space where the smaller semicircle has the same number of points, N_2.

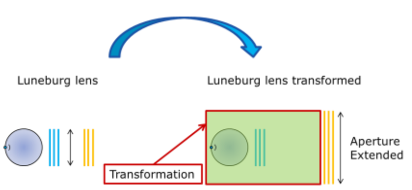

Fig. 16 Description of the problem with the lens and the space after it transformed

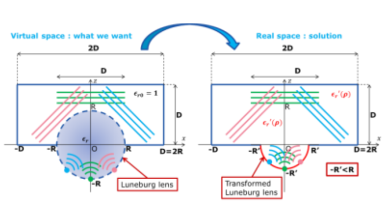

Fig. 17 T.O. structures for Luneburg lens radiating aperture extension. D = 240mm.

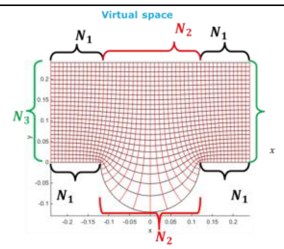

Fig. 18 Orthogonal grid of the virtual space in PointWise. $N_1 = 156, N_2 = 169, N_3 = 241$.

2. Parallel Plate Waveguide Luneburg Lens through a Holey Plate Metasurface

Introduction

A parallel plate waveguide Luneburg lens synthesized with holey plate metasurface has been designed in the scope of the collaboration between KTH and IETR started in June 2014. The lens fed by a probe has been simulated in CST and the field distribution showed good collimation of the cylindrical waves. Then a paper has been submitted to EuCAP 2015 and accepted, see section 6. The final goal of this project is to prototype the lens, and for that several types of feed and radiating flare were tested before this exchange visit without any good results in terms of reflection coefficient and radiation pattern.

Feeding optimization

During this mission, we first chose and optimized a planar feed consisting of a tapered microstrip line fed by a microstrip line, shown in **Fig. 25**, and exciting a quasi-TEM mode on its aperture. The microstrip line is fed by a Southwest endlaunch connector. Have been optimized the length of the microstrip line, the length and the angle taper of the horn, and the results are good for an aperture of 5 mm as can be seen in **Fig. 26**: less than -15 dB of reflection and less than 0.3 dB insertion loss.

Flare optimization

The optimization of the linear elongated radiating flares did not give satisfactory results because from the air gap spacing of 254µm the wave needs in one hand a smooth and long transition to go out of the lens, and in another hand a wide aperture to match the free space. So we concluded that the flare has to be divided in two parts at least. The exponential flare, given in Fig. 19, satisfies the two conditions. When excited by the feed and when the parameters *a* (6mm), *b* (24mm), and *c* (5mm) are optimized, the flare is matched between 14 GHz and 26 GHz, see **Fig. 20**.

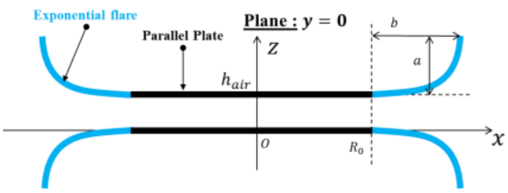

Fig. 19 Section of an exponential flare (EXP-EXP)

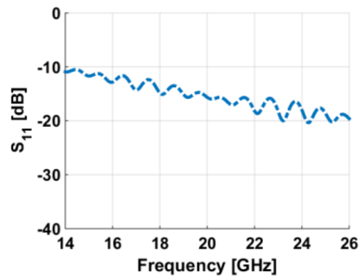

Fig. 20 Exponential flare reflection coefficient

Antenna integration and first simulations

As shown in **Fig. 20**, we integrated the feeding, the exponential flares and the metasurface. Fig. 22, Fig. 23, and Fig. 24 showed simulation results, respectively the reflection coefficient over the whole band of frequency, the gain and the amplitude of the electric field distribution at 20 GHz. The results are encouraging, 17.5 dB of gain, collimated beam, and an adaptation almost on the whole band. However, the side lobe levels were too high, i.e. more than 10dB after 18 GHz, and the S11 parameter is not under the -10 dB level around 17 GHz.

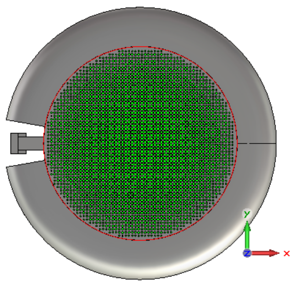

Fig. 21 Top view of the antenna

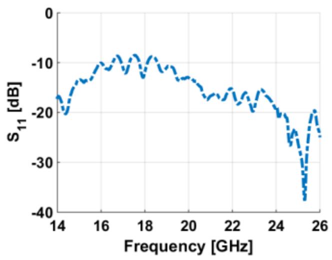

Fig. 22 Antenna S11

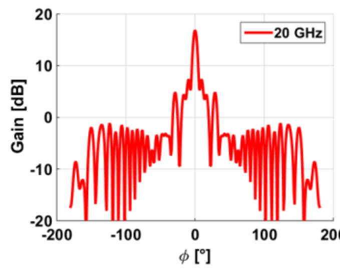

Fig. 23 Antenna gain at 20 GHz

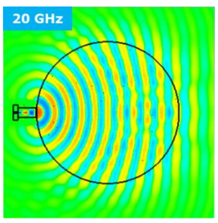

Fig. 24 Antenna E Field

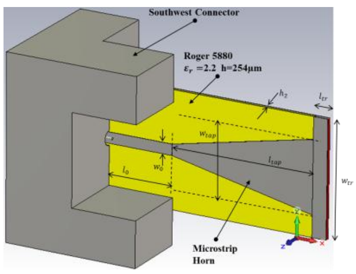

Fig. 25 Feeding structure

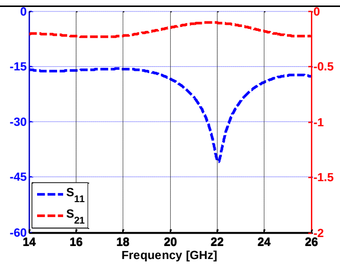

Fig. 26 Feed S parameters

Antenna optimization

Since the flare S11 parameter, **Fig. 20**, was too near the level of -10 dB from 14 GHz to 18 GHz, we decided to reduce this parameter. We started the optimization of the flare structure excited by a wave port launching a TEM mode to the PPW. By fixing the wave port aperture to 10.5mm the S11 parameter decreases of 2dB, as illustrated by the blue line in **Fig. 27**. Then we re-optimized the feed by fixing the taper aperture width at 10.5mm. Two new configurations (d03 and d07) are compared to the previous one (d02) and the simulation results shown in Fig. 29, Fig. 30, and Fig. 31. Compared to d02, d03 and d07 showed lower SLL and similar maximum gain. However the S11 parameter still needs to be reduced.

We studied the asymmetric exponential-plane flare, as shown in Fig. 32. It gives similar S11 parameter as compared to the symmetric exponential-exponential flare. So we can take advantage of its simplicity and use the asymmetric flare for manufacturing.

Future work

The antenna S11 parameter will be optimized to be less than -10 dB, a prototype will be manufactured and paper written and submitted after the measurements.

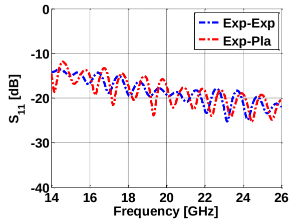

Fig. 27 S11 parameter of the two types of flares

	d02	d03	d07
w_{taper} (mm)	5	10.5	10.5
l_{taper} (mm)	10	30	30
a (mm)	6	6	6
b (mm)	24	24	24
c (mm)	5	5	5

Fig. 28 Dimensions used in d02, d03 and d07 configurations

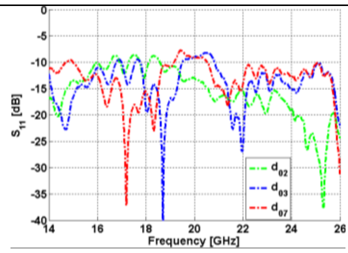

Fig. 29 S11 for of different configurations

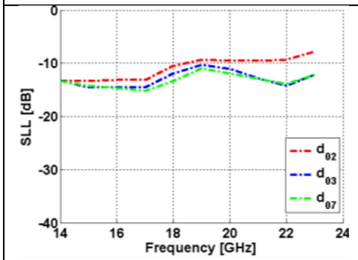

Fig. 30 SLL for of different configurations

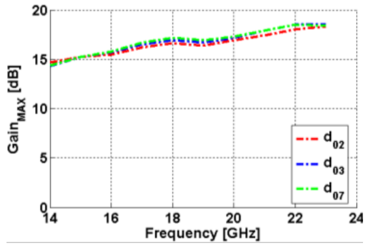

Fig. 31 GainMax for of different configurations

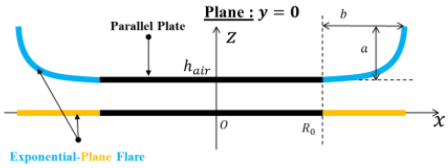

Fig. 32 Section of an hybrid flare: exponential and plane (EXP-PLA)

3. Dielectric Lens Shaping and Coma-correction zoning

Introduction

Among the several antenna solutions for MBA, the dielectric shaped[9] and coma-correction zoned[10] lens is of particular interest. Indeed, besides its low cost, light weight and high performance, it allows aperture distribution control and many special antenna patterns can be achieved. For instance, the aperture distribution control could be used to transform the cosine distribution of an H plane sectorial feed horn to get a more uniform aperture distribution.

Design procedure

During the mission, our goal was to master the design procedure then use it with transformation optics (TO) to design an innovative lens. The design procedure of the lens can be divided into four steps: (1) the power conservation law is applied to control the aperture taper; (2) Snell's law and (3) the path length constraint are applied at the boundaries of the lens; (4) The lens is zoned to reduce phase error for off-axis beams.

The code

Using the first three steps, we developed the shaping program, i.e a Matlab code in which were implemented the equations (1) to (6) of [9]. The lens shape given by the program is shown in Fig. 33. It is not the expected results, which is illustrated in Fig. 34. After debugging the code with no improvements, we decided to verify the equations of the paper.

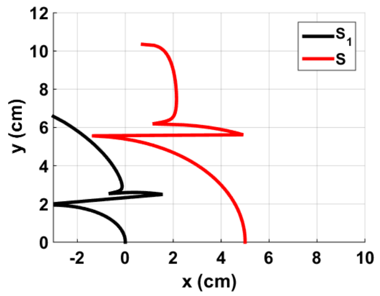

Fig. 33 Inner and outer contours of the shaped lens with the equations in [9]

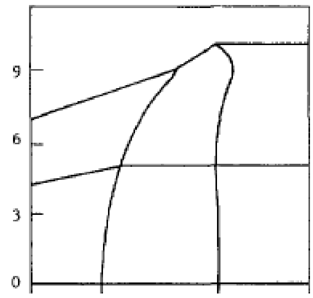

Fig. 34 Inner and outer contours of the Rexolite shaped lens [9]

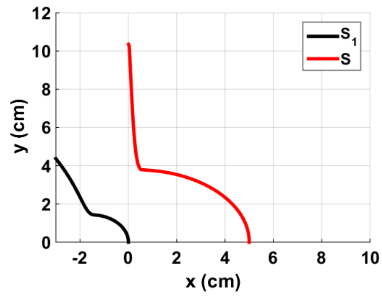

Fig. 35 Inner and outer contours of the shaped lens with the re-demonstrated equations

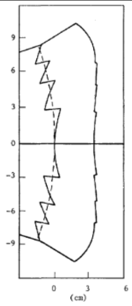

Fig. 36 A shaped lens zoned for coma reduction

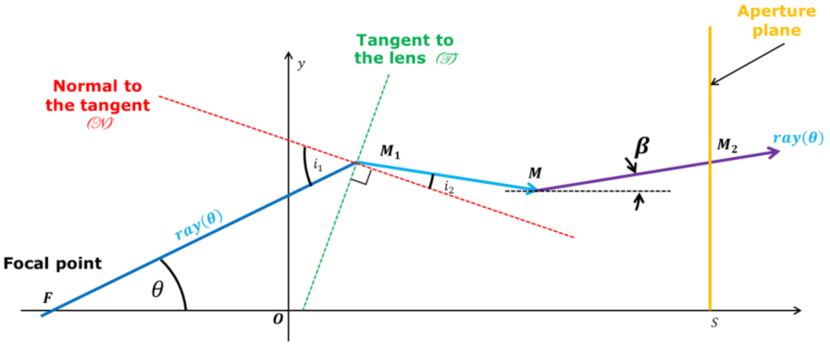

Fig. 37 Optical ray going through the lens

Equation verifications

From the optical path shown in Fig. 37, we re-demonstrated the design equations given in [9]. We found a major difference in one equation. Instead of $c = x_1^2 + (A_3^2 - A_4^2)n^{-2}$ we found $c = x_1^2 + A_3^2 - A_4^2 * n^{-2}$. By implementing this new equation, the shape given in Fig. 35 is still not the expected one. However, this shape is closer to the final one; the outer contour follows the same trend, concave then convex, as the one in Fig. 34.

Future work

To make the program work, further verifications need to be conducted, after the exchange period, on the equations and on the code, before adding the coma-correction through lens zoning, which is the next step. The complete validation of the shaping and zoning program will be effective after the full-wave simulation of the 2D lens in commercial softwares (HFSS, CST, etc). The final step will be the design of a T.O. based lens with the program.

4. CONCLUSION AND PERSPECTIVES

During this mission, first we have learned the concept and the technique of T.O. We have studied two cases found in the literature, analytical and quasi-conformal transformations. We have also flattened a parabolic reflector with T.O. reducing more 10% of space. The second step dealt with the extension of Luneburg lens radiating aperture for quasi-optical beam-forming. Because of lack of appropriate mesher and time this last task is not fully completed, but will be pursued in the frame of KTH and IETR collaboration. The final lens will be prototyped and a paper will be published.

Second, the design of PPW Luneburg lens through a holey plate metasurface has been optimized: feed and radiating flare. The beams collimates, the return loss, the side lobes and the gain are good. The return loss will be reduced before the manufacturing of the antenna. After measurements, a paper will be published.

Third, a new research topic has been investigated so it would be coupled later with T.O.: aperture distribution control. We have studied some reference papers about it, re-demonstrated the design equations and implemented them in a Matlab code. The results are not in good agreement so we think there is an error either in the equations or in the code. So the equations will be verified and the program will be debugged. When the program will be functional, the design of new lens coupled with T.O. will be considered.

Eventually, Dr. Oscar Quevedo-Teruel is planning a collaboration visit in Rennes in September 2015, so these actions will be carried on.

5. REFERENCES

[1] J. B. Pendry, D. Schurig, and D. R. Smith, "Controlling Electromagnetic Fields," *Science*, vol. 312, no. 5781, pp. 1780–1782, Jun. 2006.

[2] U. Leonhardt, "Optical Conformal Mapping and Dielectric Invisibility Devices," *arXiv:physics/0602092*, Feb. 2006.

[3] R. C. Rumpf, "Transformation Electromagnetics."

[4] J. Li and J. B. Pendry, "Hiding under the Carpet: A New Strategy for Cloaking," *Phys. Rev. Lett.*, vol. 101, no. 20, p. 203901, Nov. 2008.

[5] N. Kundtz and D. R. Smith, "Extreme-angle broadband metamaterial lens," *Nat. Mater.*, vol. 9, no. 2, pp. 129–132, Feb. 2010.

[6] "Mesh and Grid Generation Software for CFD - Pointwise." [Online]. Available: http://www.pointwise.com/pw/. [Accessed: 25-Mar-2015].

[7] M. Ettorre, R. Sauleau, and L. Le Coq, "Multi-Beam Multi-Layer Leaky-Wave SIW Pillbox Antenna for Millimeter-Wave Applications," *IEEE Trans. Antennas Propag.*, vol. 59, no. 4, pp. 1093–1100, Apr. 2011.

[8] W. Tang, Y. Hao, and F. Medina, "Broadband extraordinary transmissionin a single sub-wavelength aperture," *Opt. Express*, vol. 18, no. 16, pp. 16946–16954, Aug. 2010.

[9] J. Lee, "Dielectric lens shaping and coma-correction zoning, part I: Analysis," *IEEE Trans. Antennas Propag.*, vol. 31, no. 1, pp. 211–216, Jan. 1983.

[10] J. J. Lee and R. Carlise, "A coma-corrected multibeam shaped lens antenna, part II: Experiments," *IEEE Trans. Antennas Propag.*, vol. 31, no. 1, pp. 216–220, Jan. 1983.

6. SUBMITTED PAPERS

C.D.Diallo, O. Quevedo Teruel, G. Valerio, H. Legay, R. Sauleau, "Parallel Plate Waveguide Luneburg Lens Through a Holey Plate Metasurface", Conference EuCAP 2015, Apr 2015, Lisbonne, Portugal. 2015, 9th European Conference on Antennas and Propagation.